

Phase transitions in the spin-1/2 Heisenberg antiferromagnet on the square lattice

Jie Qiao^{1*}, Shu-Hao Zhang², Jing-Bo Qin¹, Xiao-Long Zhao¹, Qiang Cheng¹

¹School of Science, Qingdao University of Technology, Qingdao, Shandong, China

²School of Liberal Arts and Sciences, Qingdao Binhai University, Qingdao, Shandong, China

The nature of the intermediate ground-state phase in the spin-1/2 frustrated square lattice model has long been debated. Using cluster density matrix embedding theory, we investigate the phase diagram of this model. The Néel phase is directly identified for $J_2 < 0.45$ and the collinear phase for $J_2 > 0.65$ based on the ground state. Although no direct evidence of an internal phase transition is found within the intermediate phase from the ground state, analysis of the first excited state wave function reveals a continuous quantum phase transition in this region, with a critical point at $J_2 = 0.55$. This critical point divides the intermediate phase into PVBS and CVBS.

Keywords: spin-1/2, square-lattice, phase diagram, phase transition, first excited state

* Corresponding author's email: qiaojie@qut.edu.cn

1. Introduction

The exploration of quantum phases and phase transitions in strongly correlated systems has long captivated the attention of physicists [1-4]. These studies not only provide valuable insights into the fundamental behavior of matter but also reveal the exotic phenomena exhibited by these systems [5-14]. The J_1 - J_2 Heisenberg model on a square lattice is a prominent example. In the early days of high-temperature superconductivity research, the J_1 - J_2 model on a square lattice was one of the most important frustrated magnetic models, attracting significant research interest from both theoretical and experimental perspectives. Increasingly, experiments and theories indicate that real materials such as the vanadium layered oxides $Li_2VO(Si,Ge)O_4$ [15-17], the double perovskite compounds $Sr_2CuTe_{1-x}W_xO_6$ [18,19], and the polycrystalline sample $BaCdVO(PO_4)_2$ [20,21], can be adequately described by frustrated square lattice antiferromagnets with nearest-neighbor (J_1) and next-nearest-neighbor (J_2) exchanges. Frustrated square lattice systems can be described by the two-dimensional J_1 - J_2 Heisenberg model, a simple yet typical quantum spin model. The antiferromagnetic J_1 - J_2 model has been studied in detail by various methods due to its extreme importance in condensed matter physics.

Over the past three decades, the nature of the zero-temperature phase diagram of the spin-1/2 J_1 - J_2 Heisenberg model on a square lattice has been a subject of controversy and remains a fundamental unsolved problem in quantum many-body theory. For the intermediate coupling region, it has long been believed that quantum fluctuations will destroy antiferromagnetic long-range order before the maximum frustration point of the classical model at $J_2/J_1=0.5$, potentially establishing a new paramagnetic phase. The nature of this paramagnetic phase is of great interest. Various methods have been developed to study the intermediate paramagnetic phase [22-52], and different candidate ground states have been proposed, including the columnar valence bond solid (CVBS) state [22,24-26,45], the plaquette valence bond solid (PVBS) state [11,28-33,39-41,51,52], and (gapped) gapless quantum spin liquid (QSL) states [11,36,38,42,43,46-50,53-55]. However, the physical nature of the paramagnetic phase remains a mystery. These insights have been obtained through a variety of methods, including exact diagonalization [24,30,56], series expansion [26,34,57], density matrix renormalization group (DMRG) [11,36,40], (infinite) projected entangled pair states ((i)PEPS) [44,45,54,58,59], neural networks [50], and quantum Monte Carlo (QMC) [47,50,53].

A substantial body of research has been dedicated to exploring the phase diagram of the J_1 - J_2 Heisenberg model on a square lattice. This model has become a focal point in quantum magnetism research. A recent study employing the iPEPS algorithm simulated the global phase diagram of the J_1 - J_2 Heisenberg model, revealing that the non-magnetic region spans

$0.45 \leq J_2/J_1 \leq 0.61$. Within this range, it identified a gapless spin liquid phase for $0.45 \leq J_2/J_1 \leq 0.56$ and a weak valence bond solid (VBS) phase for $0.56 \leq J_2/J_1 \leq 0.61$ [54]. Subsequently, a very recent study using the DMRG and fully augmented matrix product states methods analyzed level crossings in the excitation spectrum to pinpoint phase transition points. This study found a direct phase transition between the Néel antiferromagnetic and VBS phases at $J_2/J_1=0.535(3)$, with no intermediate spin liquid phase present [60]. Additionally, several other works have suggested the existence of a phase transition in the intermediate region [11, 50, 53]. However, despite the abundance of results and analyses, the nature of the non-magnetic region within the range $0.4 \leq J_2/J_1 \leq 0.6$ remains a subject of intense debate and active research. The intermediate-phase phase transition is a continuous phase transition, which is challenging to detect in the ground state but observable in the first excited state [11, 49, 61, 62].

In this paper, we employ the Cluster Density Matrix Embedding Theory (CDMET) to calculate the ground state and first excited state of the spin-1/2 antiferromagnetic J_1 - J_2 model. The ground-state results reveal that the transition from the Néel antiferromagnetic phase to the intermediate phase is continuous, while the transition from the intermediate phase to the stripe antiferromagnetic phase is first-order. By probing the first excited state, we identify a continuous phase transition point within the intermediate phase of the ground state at $J_2=0.55$. By calculating the correlation functions, we find a valence-bond-solid (VBS) phase transition in the first excited state of the impurity clusters. As shown in **Figure 1**, we present a phase diagram for a J_1 - J_2 square lattice model.

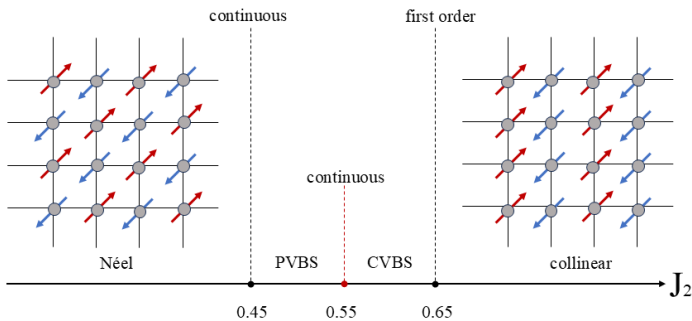


Figure 1. The phase diagram of spin-1/2 J_1 - J_2 square-lattice Heisenberg antiferromagnetic model. The system exhibits a Néel antiferromagnetic order when $J_2 < 0.45$ (continuous phase transition) and transitions to a collinear antiferromagnetic phase when $J_2 > 0.65$ (first-order phase transition). A continuous phase transition exists at $J_2=0.55$ within the intermediate region ($0.45 \leq J_2 \leq 0.65$), splitting this phase into two distinct VBS phases.

2. The J_1 - J_2 Model and CDMET Approach

The spin-1/2 J_1 - J_2 antiferromagnetic Heisenberg model is a typical model for studying the interplay between frustration effects and quantum phase transitions. It is generally established

that the ground state of this model hosts two distinct long-range ordered phases, which are separated by an intervening disordered quantum paramagnetic phase. The Hamiltonian of this model is given by the following expression

$$H = J_1 \sum_{\langle i,j \rangle} S_i S_j + J_2 \sum_{\langle\langle i,k \rangle\rangle} S_i S_k, \quad (1)$$

where S_i is the spin-1/2 operator located at site i , and the summation is performed over nearest-neighbor pairs ($\langle i,j \rangle$) and next-nearest-neighbor pairs ($\langle\langle i,k \rangle\rangle$), as shown in **Figure 2**. This model includes nearest-neighbor (J_1 , the energy unit in this work) and next-nearest-neighbor (J_2) exchange interactions, demonstrating the subtle interplay between competing magnetic interactions.

CDMET has been proven a reliable method for treating strongly correlated systems [12,63-70]. As shown in Figure 2, we divide a finite square lattice into numerous 2×2 spin clusters and arbitrarily select one cluster as the impurity cluster, with the remaining spin clusters treated as the bath state. This size and shape are chosen to maintain the equivalence of all sites within the cluster. The 2×2 spin clusters match the C_4 rotational symmetry of the Néel state and the C_2 rotational symmetry of the collinear state. Isaev et al. show that 2×2 spin clusters are suitable for the square J_1 - J_2 lattice [33]. It is clear that considering a larger spin cluster could improve the results. However, the number of bath states exponentially increases with the size of the spin cluster. Our group's previous work indicate that, unlike other simulation methods which exhibit significant size effects, the bond energy of the impurity cluster is insensitive to the lattice size [12]. This difference implies that using CDMET, we can obtain reasonable results in the thermodynamics limit by calculating only a finite lattice system.

The wave function of the 2×2 spin cluster impurity model is expressed exactly by

$$|\phi\rangle = \sum_{l=1}^{16} a_l |\mu\rangle_l |\nu_{bps}\rangle_l, \quad (2)$$

where the $\{|\nu_{bps}\rangle\}$ is 16 block-product states, which is referred to as the bath state. The approximation of the bath state is consistent with the hierarchical mean-field theory with 2×2 spin cluster. The $\{|\mu\rangle\}$ is 16 standard basis vectors and the $\{a_l\}$ represents the expansion coefficients of the wave function. We use $\|(H-E)|\phi\rangle\|^2$ to minimize the length of the state. If the wave function is accurate, the norm is zero. H , ϕ , and E represent the system's Hamiltonian, the CDMET wave function, and the target energy, respectively.

Through the variational method, we can obtain an approximate eigenstate $|\phi\rangle$ which eigenvalue is closest to E . We use the following variational prescription:

$$\frac{\partial}{\partial \phi_{i,\sigma}} \|(H - E)|\phi\rangle\|^2 \simeq 0, \quad (3)$$

where $\partial/\partial \phi_{i,\sigma}$ indicates the variation of the $|\phi\rangle$ by varying the real matrix $\phi_{i,\sigma}$ on site i and spin σ . In our previous work, we employed this method to calculate the excited states of the J1-J2 Heisenberg model at different energy levels and discovered the presence of an energy gap in the intermediate phase [68]. Therefore, based on this foundation, we can gradually approximate the first excited state using the least squares method in this study. We employ an 8×8 system with periodic boundary conditions, which has been demonstrated to closely approximate an infinite system. The computation cost is lower than that of other methods. We obtained a relative error between approximately 10^{-6} and 10^{-5} from our calculations on an 8×8 lattice system [67].

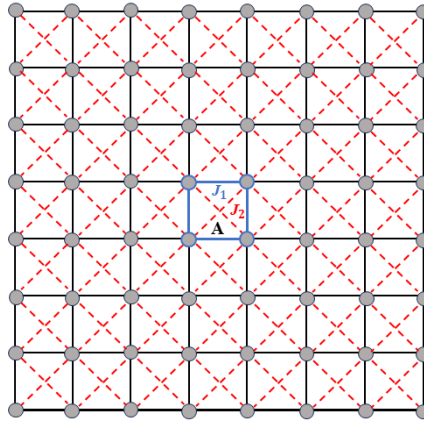


Figure 2. A lattice under periodic boundary conditions is divided into multiple 2×2 spin clusters, where one cluster (A) is regarded as an impurity cluster, and the remaining spin clusters are considered as the bath state.

3. Results and Discussion

Discontinuities or singularities in entanglement entropy signal the onset of first-order quantum phase transitions, whereas divergent peaks in entropy derivatives characterize continuous quantum phase transitions [71-76]. We calculate the single-site and four-site von Neumann entanglement entropy between the impurity cluster and its environment, as illustrated in Figure 2. When partitioning the lattice spin system into subsystem A and its complement B, the von Neumann entanglement entropy for both subsystems can be readily obtained and is defined as

$$S(\rho_A) = -Tr(\rho_A \ln \rho_A), \quad (4)$$

where $\rho_A = tr_B |\phi\rangle\langle\phi|$ is the reduced density matrix. The evolution of entanglement entropy for the ground state (see **Figure 3**) and first excited state (see **Figure 5**) is plotted against J_2 . The data series are labeled as follows: S_{GS} and S_{ES} correspond to single-site entanglement entropy,

and S_{GP} and S_{EP} to four-site entanglement entropy, for the ground and first excited states, respectively.

3.1. Directly Observable Phase Transitions in the Ground State

In Figure 3, we calculate the ground-state energy (E), entanglement entropy (S_{GS} and S_{GP}) and its first-order derivatives (S'_{GS} and S'_{GP}) as functions of J_2 . As shown in Figure 3(a), the energy E of the embedded single site exhibits a discontinuity at $J_2=0.65$. Simultaneously, both entanglement entropy curves in Figure 3(b) display discontinuities at the same critical value $J_2=0.65$, indicating a first-order phase transition at this point. Furthermore, the first derivative of the entanglement entropy, shown in Figure 3(c), captures a second-order (continuous) phase transition, with all curves exhibiting peaks at $J_2=0.45$, confirming this as a second-order phase transition point. These results are in good agreement with the results obtained by other approximations [32,39,54,77,78]. Darradi et al. used the coupled cluster method for high orders of approximation and complementary exact diagonalization in its study [32], with results indicating that the quantum critical points for both the Néel and collinear orders are $J_2^{c1} \approx (0.44 \pm 0.01)J_1$ and $J_2^{c2} \approx (0.59 \pm 0.01)J_1$, respectively. Yu et al. applied the plaquette renormalization scheme of tensor network states and observed a continuous transition between the Néel order and the plaquettelike order near $J_2^{c1} \approx 0.40J_1$, the collinear order emerges at $J_2^{c1} \approx 0.62J_1$ through a first-order phase transition [39].

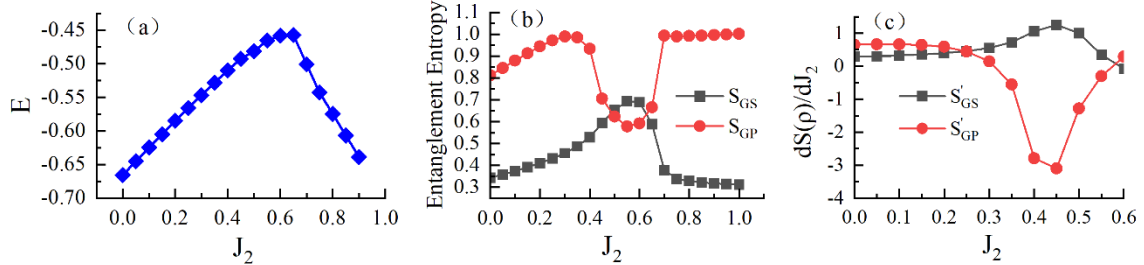


Figure 3. Panels (a), (b), and (c) show, respectively, the ground-state energy (E), entanglement entropy (S_{GS} and S_{GP}), and its first-order derivative (S'_{GS} and S'_{GP}) as functions of J_2 .

Furthermore, by calculating the spin expectation value components $\eta = (S_x, S_z)$, we obtain the spin vector diagrams shown in **Figure 4(a)** for $J_2=0.20$ and **Figure 4(b)** for $J_2=0.80$. When $J_2 < 0.45$, the spins on neighbor lattice sites are antiparallel, while those on diagonal sites are parallel, forming a staggered periodic arrangement characteristic of the Néel state, as illustrated in Figure 4(a). When $J_2 > 0.65$, the spins are aligned parallel along one crystallographic axis and antiparallel along the other, resulting in a collinear order periodic pattern, indicative of the stripe state, as shown in Figure 4(b).

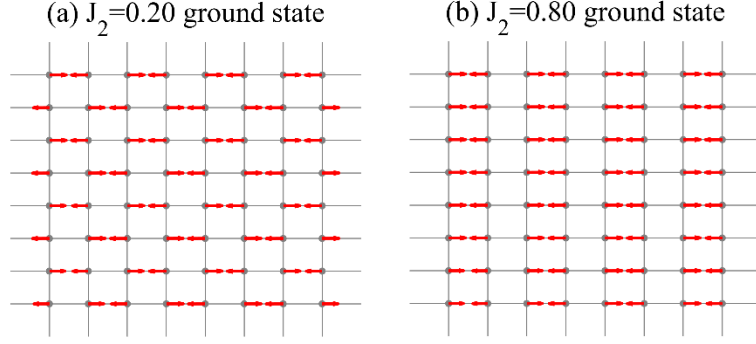


Figure 4. Vector map of the spin expectation value: distribution for the ground state at (a) $J_2=0.20$ and (b) $J_2=0.80$.

3.2. The Hidden Phase Transitions and the First Excited State

In recent years, numerous results have indicated that the intermediate phase exhibits a phase transition point [11,49,50,53,54,60]. Wang et al. use the DMRG method to identify excited-level crossings versus the coupling ratio $g = J_2/J_1$, identifying a phase transition at $g_{c2} \approx 0.52$ [11]. Similarly, Qian et al. utilize excited-level crossing analysis to pinpoint the phase transition points $J_2/J_1=0.535(3)$ [60]. Liu et al. use the finite projected entangled pair state (PEPS) algorithm to determine the three phase transition points of the ground state phase as $J_2=0.45$, $J_2=0.56$, and $J_2=0.61$ [54]. Although this phase transition is not directly observed in the ground state, the first excited state can serve as a probe for it.

We calculate the first excited state in order to determine the position of the intermediate phase transition point. We present the variation curves of entanglement entropy (Figure 5(a)), and its second derivative (Figure 5(b)) with respect to J_2 . In Figure 5(a), both the single-site entanglement entropy S_{ES} and the four-site entanglement entropy S_{EP} exhibit discontinuities near $J_2=0.55$. The second-order derivatives of these two entanglement entropies (S''_{ES} and S''_{EP}) exhibit pronounced peaks at $J_2=0.55$ (see Figure 5(b)). We determine that a continuous phase transition occurs at this point. This finding is further corroborated by the recent work of Nomura et al., who explicitly demonstrate the existence of a continuous phase transition at $J_2=0.54$ [49].

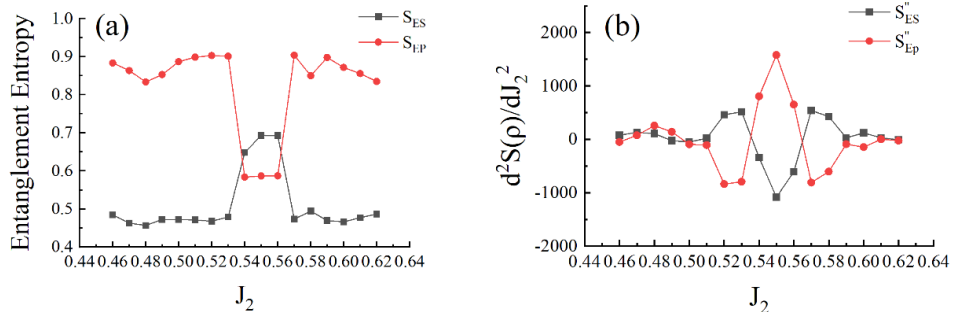


Figure 5. Panel (a) shows the entanglement entropy (S_{ES} and S_{EP}) of the first excited state as a function of J_2 . Panel (b) shows its second-order derivative (S''_{ES} and S''_{EP}) as a function of J_2 .

Numerous research findings have demonstrated evidence of the existence of a VBS phase in the intermediate phase of this system, lattice translation symmetry is spontaneously broken [26,30,33,39-41,45,60]. By computing the nearest-neighbor spin correlation functions in the first excited state, we attempt to analyze the nature of the intermediate phase. We employ exactly representable impurity clusters to demonstrate this result. **Figure 6** displays the corresponding correlation function values within impurity clusters (A) and between neighbor clusters for the first excited state. The spin-spin correlation function for neighbor spins is evaluated using

$$\xi = \langle S_i S_j \rangle, \quad (5)$$

where i and j denote neighboring spin pairs. In Figure 6, dashed lines represent intra-cluster correlations, while solid lines denote inter-cluster correlations. Line thickness reflects the correlation strength.

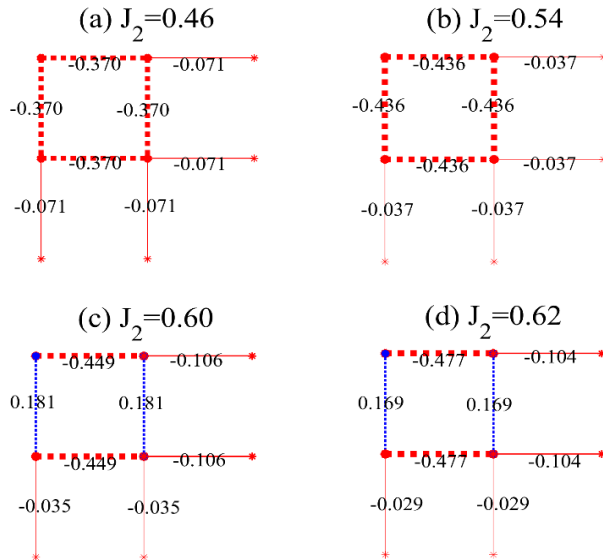


Figure 6. Correlation functions of the system's first excited state for different J_2 values. (a) $J_2=0.46$, (b) $J_2=0.54$, (c) $J_2=0.60$, (d) $J_2=0.62$. Red and blue lines represent $\xi < 0$ and $\xi \geq 0$, respectively.

As shown in Figure 6, we present the correlation functions for different values of J_2 . When $J_2=0.46$ (Figure 6(a)) and $J_2=0.54$ (Figure 6(b)), the correlation functions between nearest-neighbor sites within the clusters are equal and both negative, with values of $\xi=-0.370$ and $\xi=-0.436$, respectively. In contrast, the correlation functions between neighboring sites across clusters are also equal but relatively small in magnitude, with values of $\xi=-0.071$ and $\xi=-0.037$, respectively. These results indicate that in the range of $0.45 \leq J_2 < 0.55$, each cluster acts as a

strongly correlated unit, and the system exhibits a plaquette arrangement—a hallmark of the PVBS phase.

When $J_2=0.60$ (Figure 6(c)) and $J_2=0.62$ (Figure 6(d)), the correlation functions between nearest-neighbor sites within the clusters become unequal. The correlation functions along the Y-direction within the clusters turn positive (with values of $\xi=0.181$ and $\xi=0.169$, respectively), while those along the X-direction remain negative (with values of $\xi=-0.449$ and $\xi=-0.477$, respectively). Significant changes also occur in the correlation functions between neighboring sites across clusters: although still negative, the values along the X-direction become relatively large in magnitude (with values of $\xi=-0.106$ and $\xi=-0.104$, respectively), while those along the Y-direction become relatively small (with values of $\xi=-0.035$ and $\xi=-0.029$, respectively). In this work, the X-direction consistently refers to the horizontal direction of the lattice, and the Y-direction to the vertical direction. These results indicate that when $0.55 < J_2 \leq 0.65$, the correlation functions—both within and across clusters—exhibit distinct differences between the X and Y directions. This behavior is consistent with the CVBS phase, where valence bonds form a columnar periodic arrangement along specific crystallographic directions (either vertical or horizontal).

Although our results identify the intermediate phase as a VBS, other studies suggest it could be a Z_2 quantum spin liquid [11,36,38,42,43,46-50,53-55] characterized by weak dimerization (i.e., VBS order). This implies that the true intermediate phase may either be a coexistence state of spin liquid and VBS order, or that these two states are energetically proximate.

According to Landau's phase transition theory, the phase transition of a system corresponds to the change of its symmetry. As shown in Figure 7, the order parameters F_X and F_Y reflect the degree of bond-energy dimerization and can illustrate the change in the lattice's translational symmetry. The F_X (orange) represents the degree of dimerization along the X-direction of the lattice, while the F_Y (green) represents that along the Y-direction. These order parameters reflect the change in the system's translational symmetry. Their definition are provided in References [79,80] as:

$$F_X = \frac{1}{N} \sum_{x,y} (-1)^x S_{x,y} S_{x+1,y}, \quad F_Y = \frac{1}{N} \sum_{x,y} (-1)^y S_{x,y} S_{x,y+1}, \quad (6)$$

where x and y are coordinates of a clusters in the lattice.

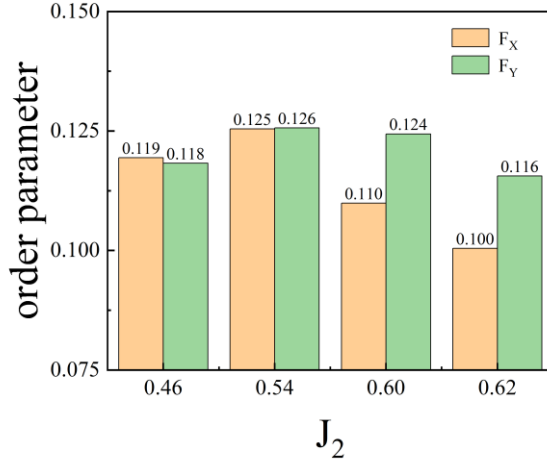


Figure 7. Comparison of order parameter values for the first excited state at different J_2 : (a) $J_2=0.46$, (b) $J_2=0.54$, (c) $J_2=0.60$, (d) $J_2=0.62$.

The variation of order parameters (F_X and F_Y) for the first excited state at different J_2 values is displayed in Figure 7. At $J_2=0.46$ and 0.54 , the order parameters F_X and F_Y are virtually identical. This indicates that the lattice retains its translational symmetry, marking the formation of an isotropic plaquette structure in the system. At $J_2=0.60$ and 0.62 , a distinct disparity emerges between the order parameters F_X and F_Y , with F_Y becoming larger than F_X . This indicates that the system exhibits significant anisotropy between the X and Y directions, implying the breaking of translational symmetry and the formation of a columnar arrangement.

4. Conclusion

In this study, we employ the CDMET method to compute the ground state and first excited state of the spin-1/2 J_1 - J_2 Heisenberg model. Analysis of the ground-state results identifies two antiferromagnetic phase transition points at $J_2 < 0.45$ (continuous phase transition) and $J_2 > 0.65$ (first-order phase transition). Within the intermediate region ($0.45 \leq J_2 \leq 0.65$), by examining the entanglement entropy of the first excited state as a function of J_2 , a continuous phase transition is identified at $J_2=0.55$. Analysis of the spin-spin correlation functions and order parameters indicates the emergence of two distinct valence-bond solid (VBS) orders in this intermediate region: the plaquette VBS (PVBS) phase and the columnar VBS (CVBS) phase.

Acknowledgements

This work was supported by the National Natural Science Foundation of China (Grant Nos. 12005110; 12474046), and the Natural Science Foundation of Shandong Province (Grant Nos. ZR2022QA110; ZR2023MA005). The numerical calculations in this work have been done on the platform in the Supercomputing Center of Wuhan University. We acknowledge useful discussions with Quanlin Jie.

Data Availability Statement

The data that support the findings of this study are available from the corresponding author upon reasonable request.

References

- [1] X.G.Wen, *Quantum Field Theory of Many-Body Systems: From the Origin of Sound to an Origin of Light and Electrons* (Oxford University Press, Oxford, 2007).
- [2] H. Fehske, R. Schneider, and A. Weiße, *Computational Many-Particle Physics* (springer, Berlin, 2008), Vol. 739.
- [3] C. Lacroix, P. Mendels, and F. Mila, *Introduction to Frustrated Magnetism* (Springer Berlin, 2011), Vol. 164.
- [4] D. C. Cabra, A. Honecker, and P. Pujol, *Modern Theories of Many-Particle Systems in Condensed Matter Physics* (springer, Berlin, 2012), Vol. 843.
- [5] Z. Fan and Q.-L. Jie, Ordered magnetic phase in a frustrated spin-½ Heisenberg antiferromagnetic stacked square lattice, *Phys. Rev. B* **89**, 054418 (2014).
- [6] Y. Cui *et al.*, Proximate deconfined quantum critical point in $\text{SrCu}_2(\text{BO}_3)_2$, *Science* **380**, 1179 (2023).
- [7] A. W. W. Ludwig, D. Poilblanc, S. Trebst, and M. Troyer, Two-dimensional quantum liquids from interacting non-Abelian anyons, *New J. Phys.* **13**, 045014 (2011).
- [8] M. Brooks, M. Lemeshko, D. Lundholm, and E. Yakaboylu, Molecular Impurities as a Realization of Anyons on the Two-Sphere, *Phys. Rev. Lett.* **126**, 015301 (2021).
- [9] N. Hiroyoshi, M. Yuki, and S. Shin-ichi, Long-Range Phase Order in Two Dimensions under Shear Flow, *Phys. Rev. Lett.* **126**, 160604 (2021).
- [10] H. Cheolhee, I. Z., K. Yaakov, A. A., P. F., M. Yigal, M. A. K., and S. Eran, Fractional Entropy of Multichannel Kondo Systems from Conductance-Charge Relations, *Phys. Rev. Lett.* **128**, 146803 (2022).
- [11] L. Wang and A. W. Sandvik, Critical Level Crossings and Gapless Spin Liquid in the Square-Lattice Spin-1/2 J_1 - J_2 Heisenberg Antiferromagnet, *Phys. Rev. Lett.* **121**, 107202 (2018).
- [12] Z. Fan and Q.-L. Jie, Cluster density matrix embedding theory for quantum spin systems, *Phys. Rev. B* **91**, 195118 (2015).
- [13] Y. Cui, R. Yu, and W. Yu, Deconfined Quantum Critical Point: A Review of Progress, *Chin. Phys. Lett.* **42**, 047503 (2025).

[14] R. Haghshenas, W.-W. Lan, S.-S. Gong, and D. N. Sheng, Quantum phase diagram of spin-1 J_1 - J_2 Heisenberg model on the square lattice: An infinite projected entangled-pair state and density matrix renormalization group study, *Phys. Rev. B* **97**, 184436 (2018).

[15] R. Melzi, P. Carretta, A. Lascialfari, M. Mambrini, M. Troyer, P. Millet, and F. Mila, $\text{Li}_2\text{VO}(\text{Si},\text{Ge})\text{O}_4$, a Prototype of a Two-Dimensional Frustrated Quantum Heisenberg Antiferromagnet, *Phys. Rev. Lett.* **85**, 1318 (2000).

[16] P. Carretta, N. P. R. Melzi, and a. a. P. Millet, Very-low-frequency excitations in frustrated two-dimensional $S=1/2$ Heisenberg antiferromagnets, *Phys. Rev. Lett.* **88**, 047601 (2002).

[17] R. Melzi, S. Aldrovandi, F. Tedoldi, P. Carretta, P. Millet, and F. Mila, Magnetic and thermodynamic properties of $\text{Li}_2\text{VOSiO}_4$: A two-dimensional $S=1/2$ frustrated antiferromagnet on a square lattice, *Phys. Rev. B* **64**, 024409 (2001).

[18] T. Koga, N. Kurita, M. Avdeev, S. Danilkin, T. J. Sato, and H. Tanaka, Magnetic structure of the $S=1/2$ quasi-two-dimensional square-lattice Heisenberg antiferromagnet $\text{Sr}_2\text{CuTeO}_6$, *Phys. Rev. B* **93**, 054426 (2016).

[19] M. Watanabe, N. Kurita, H. Tanaka, W. Ueno, K. Matsui, and T. Goto, *Valence-bond-glass state with a singlet gap in the spin-1/2 square-lattice random J_1 - J_2 Heisenberg antiferromagnet $\text{Sr}_2\text{CuTe}_{1-x}\text{W}_x\text{O}_6$* , *Phys. Rev. B* **98**, 054422 (2018).

[20] S. Meyer, B. Mertens, and H. Müller-Buschbaum, $\text{SrZn}(\text{VO})(\text{PO}_4)_2$ and $\text{BaCd}(\text{VO})(\text{PO}_4)_2$: Vanadylphosphates Related but not Isotypic to the $\text{BaZn}(\text{VO})(\text{PO}_4)_2$ Type, *Zeitschrift für Naturforschung B* **52**, 985 (1997).

[21] R. Nath, A. A. Tsirlin, H. Rosner, and C. Geibel, Magnetic properties of $\text{BaCdVO}(\text{PO}_4)_2$: A strongly frustrated spin-1/2 square lattice close to the quantum critical regime, *Phys. Rev. B* **78**, 064422 (2008).

[22] E. Dagotto and A. Moreo, Phase Diagram of the Frustrated Spin-1/2 Heisenberg Antiferromagnet in Two Dimensions, *Phys. Rev. Lett.* **63**, 2148 (1989).

[23] F. Figueirido, A. Karlhede, S. Kivelson, S. Sondhi, M. Rocek, and D. S. Rokhsar, Exact diagonalization of finite frustrated spin-1/2 Heisenberg models, *Phys. Rev. B* **41**, 4619 (1990).

[24] D. Poilblanc, E. Gagliano, S. Bacci, and E. Dagotto, Static and dynamical correlations in a spin-1/2 frustrated antiferromagnet, *Phys. Rev. B* **43**, 10970 (1991).

[25] H. J. Schulz and T. A. L. Ziman, Finite-Size Scaling for the Two-Dimensional Frustrated Quantum Heisenberg Antiferromagnet, *Europhysics Letters* **18**, 355 (1992).

[26] R. R. P. Singh, Dimer order with striped correlations in the J_1 - J_2 Heisenberg model, *Phys. Rev. B* **60**, 7278 (1999).

[27] T. Einarsson and H. J. Schulz, Direct calculation of the spin stiffness in the J_1 - J_2 Heisenberg antiferromagnet, *Phys. Rev. B* **51**, 6151 (1995).

[28] M. E. Zhitomirsky, Valence-bond crystal phase of a frustrated spin-1/2 square-lattice antiferromagnet, *Phys. Rev. B* **54**, 9007 (1996).

[29] K. i. Takano, Y. Kito, Y. Ōno, and K. Sano, Nonlinear σ Model Method for the J_1 - J_2 Heisenberg Model: Disordered Ground State with Plaquette Symmetry, *Phys. Rev. Lett.* **91**, 197202 (2003).

[30] M. Matthieu, L. Andreas, P. Didier, and M. Frédéric, Plaquette valence-bond crystal in the frustrated Heisenberg quantum antiferromagnet on the square lattice, *Phys. Rev. B* **74**, 144422 (2006).

[31] M. Arlego, Plaquette order in the J_1 - J_2 - J_3 model: Series expansion analysis, *Phys. Rev. B* **78**, 224415 (2008).

[32] R. Darradi, O. Derzhko, R. Zinke, J. Schulenburg, S. E. Krüger, and J. Richter, Ground state phases of the spin-1/2 J_1 - J_2 Heisenberg antiferromagnet on the square lattice: A high-order coupled cluster treatment, *Phys. Rev. B* **78**, 214415 (2008).

[33] L. Isaev, G. Ortiz, and J. Dukelsky, Hierarchical mean-field approach to the J_1 - J_2 Heisenberg model on a square lattice, *Phys. Rev. B* **79**, 024409 (2009).

[34] J. Sirker, Z. Weihong, O. P. Sushkov, and J. Oitmaa, J_1 - J_2 model: First-order phase transition versus deconfinement of spinons, *Phys. Rev. B* **73**, 184420 (2006).

[35] J. Richter and J. Schulenburg, The spin-1/2 J_1 - J_2 Heisenberg antiferromagnet on the square lattice: Exact diagonalization for $N=40$ spins, *Eur. Phys. J. B* **73**, 117 (2009).

[36] J. Hong-Chen, Y. Hong, and B. Leon, Spin liquid ground state of the spin-1/2 square J_1 - J_2 Heisenberg model, *Phys. Rev. B* **86**, 024424 (2012).

[37] F. Mezzacapo, Ground-state phase diagram of the quantum J_1 - J_2 model on the square lattice, *Phys. Rev. B* **86**, 045115 (2012).

[38] L. Wang, D. Poilblanc, Z.-C. Gu, X.-G. Wen, and F. Verstraete, Constructing a Gapless Spin-Liquid State for the Spin-1/2 J_1 - J_2 Heisenberg Model on a Square Lattice, *Phys. Rev. Lett.* **111**, 037202 (2013).

[39] J.-F. Yu and Y.-J. Kao, Spin-1/2 J_1 - J_2 Heisenberg antiferromagnet on a square lattice: A plaquette renormalized tensor network study, *Phys. Rev. B* **85**, 094407(6) (2012).

[40] S.-S. Gong, W. Zhu, D. N. Sheng, O. I. Motrunich, and M. P. A. Fisher, Plaquette ordered phase and quantum phase diagram in the spin-1/2 J_1 - J_2 square Heisenberg model, *Phys. Rev. Lett.* **113**, 027201 (2014).

[41] R. L. Doretto, Plaquette valence-bond solid in the square-lattice J_1 - J_2 antiferromagnet Heisenberg model: A bond operator approach, *Phys. Rev. B* **89**, 104415 (2014).

[42] Y. Qi and Z.-C. Gu, Continuous phase transition from Néel state to Z_2 spin-liquid state on a square lattice, *Phys. Rev. B* **89**, 235122 (2014).

[43] R. Johannes, Z. Ronald, and F. D. J. J., The spin-1/2 square-lattice J_1 - J_2 model: the spin-gap issue, *Eur. Phys. J. B* **88**, 2 (2015).

[44] L. Wang, Z.-C. Gu, F. Verstraete, and X.-G. Wen, Tensor-product state approach to spin-1/2 square J_1 - J_2 antiferromagnetic Heisenberg model: Evidence for deconfined quantum criticality, *Phys. Rev. B* **94**, 075143 (2016).

[45] R. Haghshenas and D. N. Sheng, U(1)-symmetric infinite projected entangled-pair states study of the spin-1/2 square J_1 - J_2 Heisenberg model, *Phys. Rev. B* **97**, 174408 (2018).

[46] W.-Y. Liu, S. Dong, C. Wang, Y. Han, H. An, G.-C. Guo, and L. He, Gapless spin liquid ground state of the spin-1/2 J_1 - J_2 Heisenberg model on square lattices, *Phys. Rev. B* **98**, 241109 (2018).

[47] W.-J. Hu, F. Becca, A. Parola, and S. Sorella, Direct evidence for a gapless Z_2 spin liquid by frustrating Néel antiferromagnetism, *Phys. Rev. B* **88**, 060402 (2013).

[48] D. Poilblanc and M. Mambrini, Quantum critical phase with infinite projected entangled paired states, *Phys. Rev. B* **96**, 014414 (2017).

[49] Y. Nomura and M. Imada, Dirac-Type Nodal Spin Liquid Revealed by Refined Quantum Many-Body Solver Using Neural-Network Wave Function, Correlation Ratio, and Level Spectroscopy, *Phys. Rev. X* **11**, 031034 (2021).

[50] S. Morita, R. Kaneko, and M. Imada, Quantum Spin Liquid in Spin 1/2 J_1 - J_2 Heisenberg Model on Square Lattice: Many-Variable Variational Monte Carlo Study Combined with Quantum-Number Projections, *J. Phys. Soc. Jpn.* **84**, 024720 (2015).

[51] Y.-H. Chan, H.-C. Jiang, and Y.-C. Chen, Plaquette valence bond state in the spin-1/2 J_1 - J_2 XY model on the square lattice, *Phys. Rev. B* **107**, 214402 (2023).

[52] L. Capriotti and S. Sorella, Spontaneous Plaquette Dimerization in the J_1 - J_2 Heisenberg Model, *Phys. Rev. Lett.* **84**, 3173 (1999).

[53] F. Ferrari and F. Becca, Gapless spin liquid and valence-bond solid in the J_1 - J_2 Heisenberg model on the square lattice: Insights from singlet and triplet excitations, *Phys. Rev. B* **102**, 014417 (2020).

[54] W.-Y. Liu, S.-S. Gong, Y.-B. Li, D. Poilblanc, W.-Q. Chen, and Z.-C. Gu, Gapless quantum spin liquid and global phase diagram of the spin-1/2 J_1 - J_2 square antiferromagnetic Heisenberg model, *Science Bulletin* **67**, 1034 (2022).

[55] T. Li, F. Becca, W. Hu, and S. Sorella, Gapped spin-liquid phase in the J_1 - J_2 Heisenberg model by a bosonic resonating valence-bond ansatz, *Phys. Rev. B* **86**, 075111 (2012).

[56] D. Elbio and M. Adriana, Phase diagram of the frustrated spin-1/2 Heisenberg antiferromagnet in 2 dimensions, *Physical Review Letters* **63**, 2148 (1989).

[57] J. Oitmaa and Z. Weihong, Series expansion for the J_1 - J_2 Heisenberg antiferromagnet on a square lattice, *Phys. Rev. B* **54**, 3022 (1996).

[58] J. Hasik, D. Poilblanc, and F. Becca, Investigation of the Néel phase of the frustrated Heisenberg antiferromagnet by differentiable symmetric tensor networks, *SciPost Phys.* **10**, 012 (2021).

[59] L. Vanderstraeten, L. Burgelman, B. Ponsioen, M. V. Damme, B. Vanhecke, P. Corboz, J. Haegeman, and F. Verstraete, Variational methods for contracting projected entangled-pair states, *Phys. Rev. B* **105**, 195140 (2022).

[60] X. Qian and M. Qin, Absence of spin liquid phase in the J_1 - J_2 Heisenberg model on the square lattice, *Phys. Rev. B* **109**, L161103 (2024).

[61] M. A. Caprio, P. Cejnar, and F. Iachello, Excited state quantum phase transitions in many-body systems, *Ann. Phys.* **323**, 1106 (2008).

[62] D. Rubeni, J. Links, P. S. Isaac, and A. Foerster, Two-site Bose-Hubbard model with nonlinear tunneling: Classical and quantum analysis, *Phys. Rev. A* **95** (2017).

[63] G. Knizia and G. K.-L. Chan, Density matrix embedding: A simple alternative to dynamical mean-field theory, *Phys. Rev. Lett.* **109**, 186404 (2012).

[64] I. W. Bulik, G. E. Scuseria, J. Dukelsky, and Density matrix embedding from broken symmetry lattice mean fields, *Phys. Rev. B* **89**, 035140 (2014).

[65] Q. Chen, G. H. Booth, S. Sharma, G. Knizia, and G. K.-L. Chan, Intermediate and spin-liquid phase of the half-filled honeycomb Hubbard model, *Phys. Rev. B* **89**, 165134 (2014).

[66] Y.-Z. Ren, N.-H. Tong, and X.-C. Xie, Cluster mean-field theory study of J_1 - J_2 Heisenberg model on a square lattice, *J. Phys.: Condens. Matter* **26**, 115601 (2014).

[67] J. Qiao and Q.-L. Jie, Density matrix embedding theory of excited states for spin systems, *Comput. Phys. Commun.* **261**, 107712 (2021).

[68] J. Qiao and Q.-L. Jie, Detection of Quantum Phase Transition by Excited State, *J. Phys. Soc. Jpn.* **90**, 094705 (2021).

[69] M. Kawano and C. Hotta, Comparative study of the density matrix embedding theory for Hubbard models, *Phys. Rev. B* **102**, 235111 (2020).

[70] X. Plat and C. Hotta, Entanglement spectrum as a marker for phase transitions in the density embedding theory for interacting spinless fermionic models, *Phys. Rev. B* **102**, 140410(R) (2020).

[71] J.-L. Song, S.-J. Gu, and H.-Q. Lin, Quantum entanglement in the S=1 / 2 spin ladder with ring exchange, *Phys. Rev. B* **74**, 155119 (2006).

[72] P. Lou and J. Y. Lee, Block-block entanglement and quantum phase transition in the spin-1/2 XX chain, *Phys. Rev. B* **74**, 134402 (2006).

[73] S.-S. Deng, S.-J. Gu, and H.-Q. Lin, Block-block entanglement and quantum phase transitions in the one-dimensional extended Hubbard model, *Phys. Rev. B* **74**, 045103 (2006).

[74] G. Vidal, J. I. Latorre, E. Rico, and A. Kitaev, Entanglement in quantum critical phenomena, *Phys. Rev. Lett.* **90**, 227902 (2003).

[75] O. Legeza and J. Solyom, Two-site entropy and quantum phase transitions in low-dimensional models, *Phys. Rev. Lett.* **96**, 116401 (2006).

[76] J. Ren and S. Zhu, Quantum phase transition in easy-axis antiferromagnetic Heisenberg spin-1 chain, *Phys. Rev. A* **79**, 034302 (2009).

[77] J. Richter, R. Darradi, J. Schulenburg, D. Farnell, and H. Rosner, Frustrated spin-1/2 J_1 - J_2 Heisenberg ferromagnet on the square lattice studied via exact diagonalization and coupled-cluster method, *Phys. Rev. B* **81**, 174429 (2010).

[78] T. Senthil, A. Vishwanath, L. Balents, S. Sachdev, and M. P. A. Fisher, Deconfined Quantum Critical Points, *Science* **303**, 1490 (2004).

[79] T. Senthil, L. Balents, S. Sachdev, A. Vishwanath, and M. P. A. Fisher, Quantum criticality beyond the Landau-Ginzburg-Wilson paradigm, *Physical Review B* **70** (2004).

[80] L. Isaev, G. Ortiz, and J. Dukelsky, Hierarchical mean-field approach to the J_1 - J_2 Heisenberg model on a square lattice, *Physical Review B* **79**, 024409 (2009).